ChemPubSoc Europe

DOI: 10.1002/batt.201900164

BATTERIES & SUPERCAPS
Articles

Phosphaviologen-Based Pyrene-Carbon Nanotube Composites for Stable Battery Electrodes

Colin R. Bridges[+],[a] Monika Stolar[+],[a] and Thomas Baumgartner*[a]

The adoption of intermittent renewable power sources has placed battery technologies into the limelight, initiating a push to develop sustainable materials for energy storage that do not rely on rare or toxic elements. Organic electrode materials are made from abundant elements that are consumed in the biomass cycle, which can make large-scale manufacturing and recycling of these materials less detrimental to the environment. Herein, we explore how organic, electroactive phosphoryl-bridged viologens (phosphaviologens) can be composited with single-walled carbon nanotubes (SWCNTs) and used as organic electrodes composed of sustainable/abundant materials. To this end, we have functionalized phosphaviologens that exhibit two stable and reversible reductions with pendant pyrene moieties to interface them with carbon nanotubes. The anchoring of the redox active species on the surface of SWCNTs prevents electrode dissolution, and hybrid batteries with a high voltage (1.95–3.5 V) vs. Li/Li^+ using phosphaviologens as the cathode remain stable past 500 charge/discharge cycles.

1. Introduction

Solar and wind energy have emerged as viable solutions for grid-scale renewable energy, however, integrating these intermittent power sources into power grids poses challenges beyond generating electricity. Energy-storage methods that use sustainable, abundant, non-toxic elements must be developed to make widespread adoption of these technologies environmentally viable. Lithium-ion batteries dominate the current research literature due to their outstanding energy density and high voltage. While Li is only moderately abundant and not considered highly toxic, Li-ion batteries use heavy-metal based inorganic electrodes, generating significant concern over the elemental abundance and environmental impact of the extraction and disposal of these materials.[1,2] Apart from this challenge, rigid and inelastic inorganic electrodes are poor materials to manage the swelling and contraction associated with charging and discharging. Swelling inorganic lattices generates significant amounts of heat, therefore discharging rates must be limited for safety reasons and to prevent degradation. Capacity fading is typically observed as the mechanical forces degrade the electrode structure.[3–6] For these reasons, mechanically resilient and environmentally benign electrode materials are highly sought after.

It is in this context that electrode materials based on carbon, nitrogen, oxygen, sulfur, and phosphorus are increasingly being evaluated as alternatives for use in Li-ion batteries.[7–9] Electrodes made from abundant elements, or elements which are consumed in the biomass cycle, make recycling or disposal more environmentally friendly.[1,2] In addition, organic materials are held together with weaker non-covalent interactions and van der Waals forces, thus they do not generate significant heat or degrade upon swelling and higher charge/discharge rates can be safely achieved.[10–13] For these reasons, organic electrode materials are considered to be extremely promising materials for sustainable batteries with high power capabilities.

While organic electrodes are potentially advantageous, there are issues that plague their performance and prevent their widespread adoption in commercial batteries. These issues include lower cycle stability due to degradation or dissolution upon repeated oxidation or reduction, self-discharge due to organic small molecules solubilizing in the electrolyte, the lower conductivity of organic materials lowering discharge rates, and low voltages due to the difficulty in finding carbon-based materials with a high reduction potential relative to lithium.[7–9,14,15]

These issues can be mitigated to some extent by judicious optimization, as molecular structures can be optimized to improve operating voltage and redox stability.[16,17] Electrode dissolution can be reduced by choosing appropriate solvents, electrolytes, and electrode binders, while conductive additives improve the conductivity of organic electrodes.[18] The results of these strategies are encouraging and molecular design strategies that improve the voltage, stability, and rate performance of organic electrodes should be explored further to fully capitalize on the synthetic variety available for organic materials.

There is a large body of literature developing organic moieties to use in electrode materials, however, relatively few classes of moieties possess discharge voltages greater than 3.0 V *versus* Li/Li^+.[7,17,19] Currently, nitroxide based radicals,[20–23] sulfur and nitrogen containing heteroaromatics,[24–27] and aromatic quinones[19,28–31] are promising molecular architectures

[a] *Dr. C. R. Bridges,[+] Dr. M. Stolar,[+] Prof. Dr. T. Baumgartner*
Department of Chemistry
York University
Toronto, ON M3J 1P3, Canada
E-mail: tbaumgar@yorku.ca

[+] *These authors contributed equally to this work.*

Supporting information for this article is available on the WWW under https://doi.org/10.1002/batt.201900164

that exhibit high voltages in Li-ion batteries, but more suitable moieties and functional groups need to be developed to achieve organic batteries having high energy and power densities. Molecular design motifs that allow electroactive organic molecules to better interface with conductive additives would prevent electrode dissolution and increase conductivity, potentially increasing stability and rate performance.

Herein, we synthesize novel phosphoryl-bridged viologens (phosphaviologens) having molecular structures designed to improve two key shortcomings with organic electrode materials: i) low voltages *vs.* Li/Li^+, and ii) electrode dissolution. The phosphaviologen scaffold has a low lying LUMO level due to both the electron-withdrawing pyridine moieties and the phosphoryl group, allowing them to operate with high voltage *vs.* Li/Li^+. In addition, the aromatic nitrogen atoms can be used as a synthetic handle to attach functional groups *via* quaternization, imparting specific material properties. We take advantage of this by coupling pyrene pendants to the phosphaviologen core allowing the small molecule to physisorb to single-walled carbon nanotubes (SWCNTs), which is expected to prevent electrode dissolution.[32] As a result, these electrodes have high voltages relative to Li/Li^+ and possess high cycle stability.

2. Results and Discussion

2.1. Design and Synthesis

The electroactive phosphaviologen core was synthesized using our previously reported procedures.[33–35] 1-(Bromomethyl)pyrene was used as a quaternizing agent to synthesize pyrene-functionalized phosphaviologen (**PY_2PV**), and the bromide counterion was exchanged for the more electrochemically stable triflate anion by treating the product with an excess of methyl triflate (Figure 1). **PY_2PV** was purified by placing the solid under vacuum remove methyl bromide and excess methyl triflate, then filtering and rinsing with acetone to yield a red solid. The final product exhibits ^1H NMR shifts between $\delta = 9.6$–8.2 ppm characteristic of viologen, a singlet observed in ^{31}P NMR ($\delta = 28.6$ ppm) characteristic of the phosphoryl-containing fused ring system, and a singlet observed in ^{19}F NMR ($\delta =$ 77.30 ppm) indicating a triflate anion. **PY_2PV** effectively formed composites with SWCNTs by mixing the desired ratio of **PY_2PV** and SWCNT together in acetonitrile, removing the solvent, followed by washing the powder with ethanol to remove any unbound molecular **PY_2PV**.

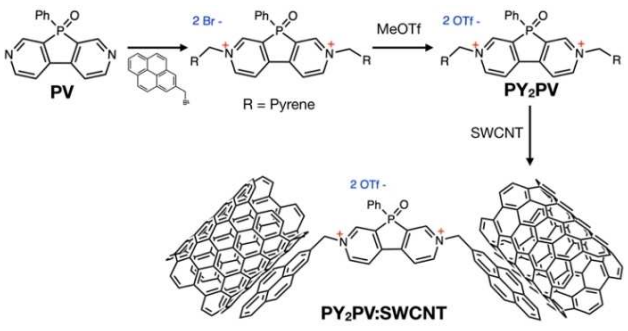

Figure 1. Synthesis of pyrene-functionalized phosphaviologens and their subsequent composite formation with SWCNTs.

Viologens and viologen derivatives have been used as electron acceptors in organic electrode materials thanks to their highly reversible reductions.[33,36–43] Often only the first reduction is used, however, viologens can act as two-electron acceptors when both reductions are reversible.[36,38,39,42,43] Phosphaviologens exhibit the stable and reversible redox behavior of viologens, while the electron-withdrawing phosphoryl unit lowers the LUMO allowing them to operate at higher voltages *vs.* Li/Li^+. The low-lying LUMO also enables phosphaviologens to stably and reversibly accept two electrons, considerably increasing the battery energy and capacity compared to alkyl viologens only using the first reduction.

It is well established that pyrene strongly interacts with SWCNTs through π-stacking,[44–46] which we can take advantage of in two ways: i) the pyrene-SWCNTs interactions will prevent phosphaviologen from dissolving into the electrolyte and ii) directly coupling the electroactive species to the conductive additive may also improve electron transfer. Combined, the phosphaviologen core with pendant pyrene groups (**PY_2PV**) is a small molecule that can act as a multiple-electron acceptor with high voltage to Li/Li^+ and can be composited with highly insoluble but electrically conducting SWCNTs. This **PY_2PV**:SWCNT composite is designed to address several problems associated with organic battery electrodes made of small molecules: the relatively low operating voltages of organic materials, and the long term capacity decay due to electrode dissolution.

2.2. Optical Properties

Absorption spectroscopy indicates that the pyrene units interact with the SWCNTs in the composite, and that there is charge transfer between the pendant pyrene groups and the phosphaviologen core (Figure 2). Phosphaviologens have rich interconnected optical and electronic properties, with the dication species having strong absorbances observed at $\lambda_{max} =$ 350 nm, 275 nm, and 220 nm, and the radical cation having strong absorbances around $\lambda_{max} = 500$–700 nm. While pure phosphaviologens show no absorbances in the visible range as a dicationic species, the **PY_2PV**:SWCNT composite shows a weak absorbance at $\lambda_{max} = 550$–650 nm (Figure 2). This absorbance matches the singly-reduced form of the phosphaviologen core observed in previous spectro-electrochemical experiments, indicating slight charge transfer from the pyrene to the viologen core that is not observed with other substituents like methyl or phenyl.[34,35] Optical spectroscopy illuminates the interactions with SWCNT, as a 0.0033 mg/mL solution of the **PY_2PV**:SWCNT composite has its absorbances between $\lambda_{max} =$ 200–400 nm reduced by 75% when compared to a solution of **PY_2PV** of identical **PY_2PV** content. The diminishing absorbance of **PY_2PV** suggests that the SWCNTs remove **PY_2PV** from

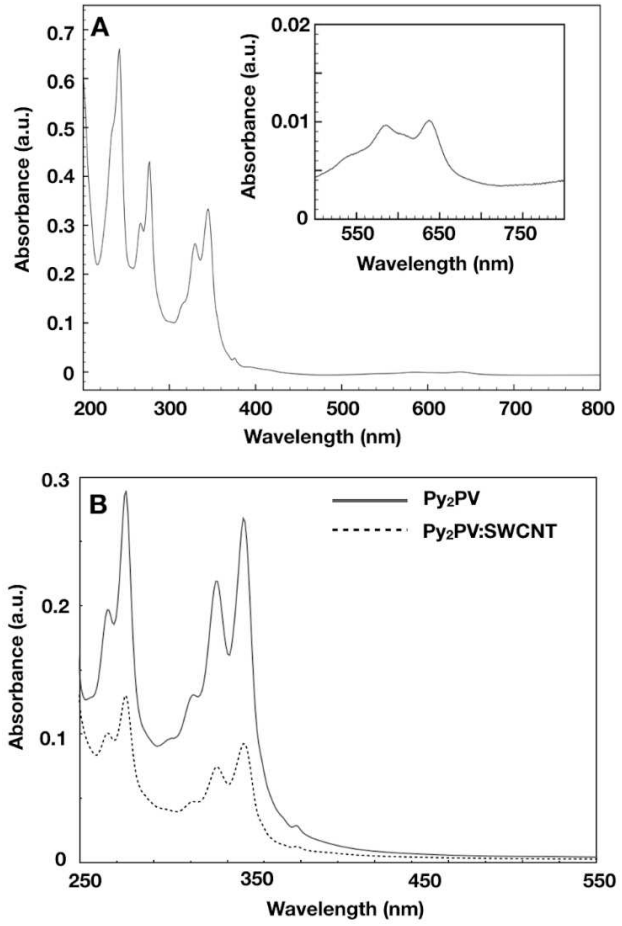

Figure 2. A) Absorbance spectroscopy on **PY_2PV** as a solution in acetonitrile (0.05 mg/mL). The weak absorbances at 600 nm (inset) are attributed to charge transfer between the phosphaviologen core and the pendant pyrene units. B) Absorbance spectroscopy on **PY_2PV** as a solution in ethanol (0.03 mg/mL) by itself (solid line) and as a 1:2 composite with SWCNT (dashed line) after filtering. The absorbances due to pyrene are reduced significantly, indicating filtering the SWCNT from solution also removes bound **PY_2PV**, showing evidence of complexation.

solution by affixing it onto the precipitate, evidence for the strong association between pyrene and the SWCNTs (Figure 2). A similar result is observed when the counter ion is exchanged for the PF_6 anion used in the battery electrolyte (Supporting Information). The electron transfer from pyrene to phosphaviologen, and the phosphaviologen interactions with SWCNT indicate this composite may be an effective material for redox-driven charge transfer in the solid-state required in electrodes.

2.3. Electrochemical Properties

Like other related phosphaviologens,[33–35] **PY_2PV** exhibits the highly reversible reductions and low-lying LUMO desired for materials in organic battery electrodes. Cyclic voltammetry on **PY_2PV** shows two reversible reductions occurring at −0.1 V and −0.5 V vs. Ag/Ag^+ with the position and shape of these peaks showing little dependency on scan rate, behavior typical of fast and reversible redox kinetics. This corresponds to charging/discharging reactions that happen at 3.2–2.8 V vs. Li/Li^+, a relatively high voltage for organic materials.[7–9,18,19] The **PY_2PV**:SWCNT composite shows the same electrochemical behavior, indicating that pyrene interactions with SWCNTs do not impact the favorable electrochemical properties of **PY_2PV** (Figure 3). The **PY_2PV**:SWCNT composite exhibits rapid and reversible electrochemical properties, and should form intimate phosphaviologen-carbon nanotube networks that facilitate electron transport in the solid state. These properties make this composite potentially interesting materials as fully organic electrodes for rechargeable batteries.

2.4. Battery Testing

The electron-withdrawing phosphaviologen and pyrene substituents allow Li-**PY_2PV**:SWCNT batteries to exhibit high voltages vs Li/Li^+ and retain their performance after 500 cycles. We fabricated hybrid inorganic-organic batteries using a Li-metal anode and an organic cathode made from the **PY_2PV**:

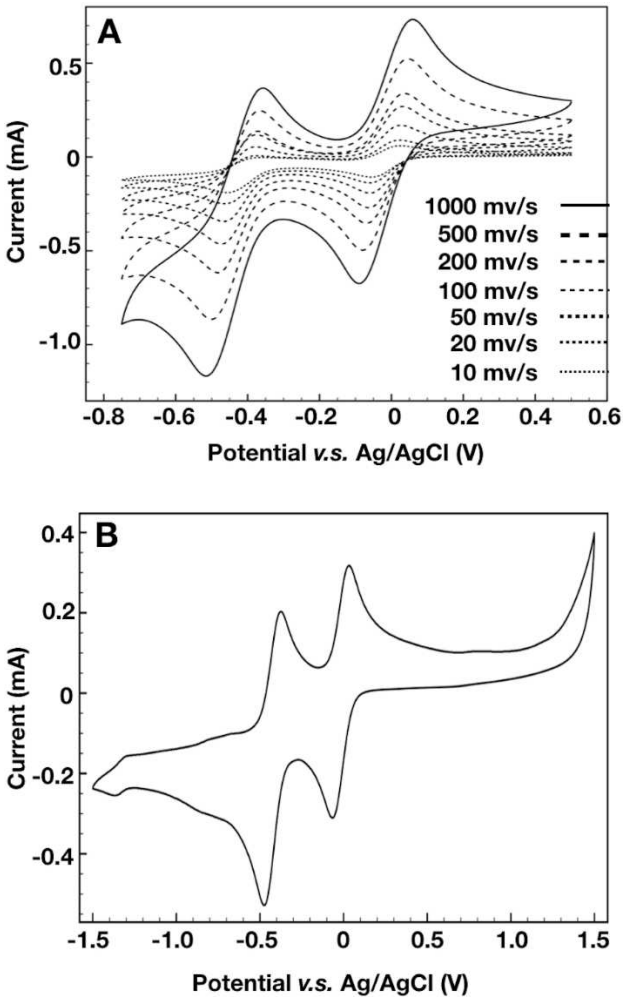

Figure 3. Cyclic voltammetry on A) **PY_2PV** at various scan rates; and B) **PY_2PV**:SWCNT composite at 10 mV/s as a solution in acetonitrile (10 mg/mL) using a 0.1 M $TBAPF_6$ supporting electrolyte. **PY_2PV** shows two reversible reductions as a solution and as a composite with SWCNT.

SWCNT composite in a 1:2 ratio, and tested the electrochemical properties using a standard coin-cell architecture. The batteries were charged and discharged between 1.95–3.5 V vs. Li/Li^+ and cycled at rates between 1 C and 20 C. This voltage range was chosen to include the full redox reaction of **PY_2PV** but to avoid irreversible reductions seen below 1.8 V and irreversible oxidation of pyrene seen around 4 V vs. Li/Li^+ (Supporting Information). The 1:2 **PY_2PV**:SWCNT composite exhibits a capacity of 48 mAh/g at 1 C, representing 90% of its theoretical capacity (53 mAh/g based off the molecular mass of 1007 g/mol), assuming phosphaviologen accepts two electrons. The reductions of **PY_2PV** are only separated by 0.4 V making it difficult to distinguish distinct plateaus on the charging profile, instead we observe a single plateau between 3.1 and 3.5 V vs. Li/Li^+. We attribute this plateau to the charging of **PY_2PV** from the neutral species to the dication. Cyclic voltammetry on the assembled battery shows much broader peaks between 3–3.5 V vs. Li/Li^+ when charging and 3.1–2.0 V vs. Li/Li^+ when discharging (Supporting Information), an indication of slow ion or electron conductivity through the solid-state electrode. This contributes to the sloped charging plateau between 3.1 and 3.5 V vs. Li/Li^+ and the slanted discharge curve mostly appearing between 3.3 and 2.1 V vs. Li/Li^+ (Figure 4).

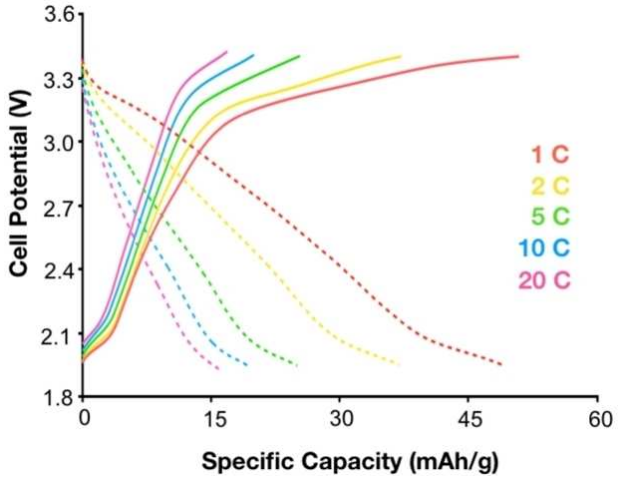

Figure 4. Charge-discharge profiles at varying C-rates for Li-ion batteries fabricated using 1:2 **PY_2PV**:SWCNT composites as the cathode. Batteries were tested in a coin cell geometry using a lithium reference and 1.0 M $LiPF_6$ in TEGDME electrolyte.

These electrodes retain more than 30% of their original capacity and maintain high coulombic efficiency at extremely high charging/discharging rates of 20 C. The capacity of the electrodes decreases at higher rates; however, the capacity completely recovers when the rate is returned to 1 C, indicating that the fast charge and discharge cycles do not cause degradation of the electrodes after 120 scans at varying C rates (Figure 5).

The 1:2 **PY_2PV**:SWCNT composite also exhibits excellent stability to repeated charging and discharging, showing no capacity fading over 500 cycles at 1 C. Indeed, the capacity increases slightly from 48 mAh/g to 53 mAh/g, a result we attribute to electrode conditioning over repeated cycling (Figure 6). Ultimately, the electrodes display high material usage, capacity retention at high C rates, and high cycle stability; all properties we can attribute to the **PY_2PV**:SWCNT composite. The physisorption of the pyrene groups to the SWCNTs provides good mixing between electroactive phosphaviologen with the conductive additive, allowing most of the material to be used during charging/discharging. Moreover, the close interfacing of the phosphaviologen cores with the SWCNTs provides efficient conduction pathways throughout the electrode, giving rise to high rate capabilities. Finally, we attribute the high cycle stability to both the strong interaction between the pyrene units and the SWCNTs that prevent electrode dissolution and the high electrochemical stability of the phosphaviologen core.

Electrodes fabricated using different ratios of **PY_2PV**:SWCNT exhibit qualitatively the same behavior; they show moderate capacity fading upon increasing rates and high to cycling at

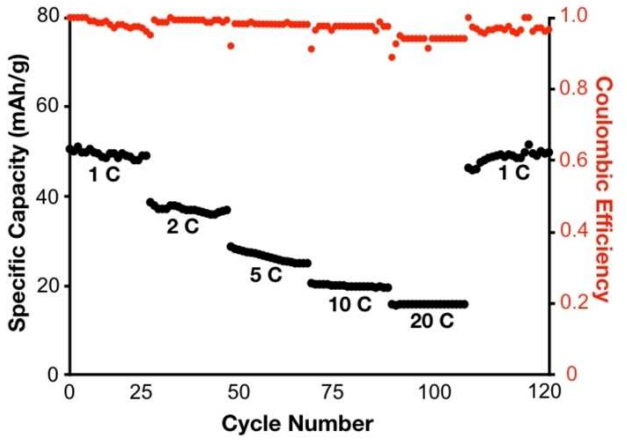

Figure 5. Capacity at varying C-rates for Li-ion batteries fabricated using 1:2 **PY_2PV**:SWCNT composites as the cathode. These composite electrodes maintain more than 30% of their capacity even at very high charging and discharging rates and display little capacity decay after 120+ cycles, while maintaining high coulombic efficiencies.

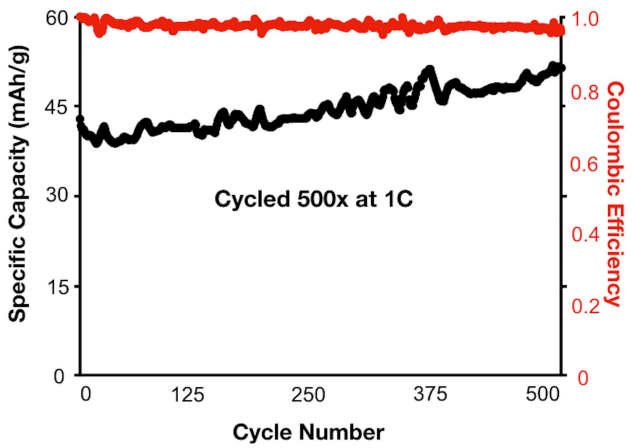

Figure 6. Cycling stability for the 1:2 **PY_2PV**:SWCNT composite at 1 C. After 500 cycles the battery capacity slightly improves to 50 mAh/g, corresponding to 94% of its theoretical capacity, and maintains a high coulombic efficiency throughout the experiment.

1 C. Our charge-discharge tests showed more significant capacity decay when discharging at 5 C over 500 cycles, a result we attribute to lower conductivity of the charged electrode and incomplete discharging at such high rates. We found that lower incorporation of SWCNT generally led to lower material usage. Since all the electrodes had similar resistance, we attribute this result to the SWCNTs becoming "saturated" in phosphaviologen, with excess phosphaviologen becoming electrically isolated from the conductive additive and ultimately not contributing to battery capacity (Supporting Information).

To further understand the impact of the pyrene functional groups and the SWCNT have on battery performance, we constructed several control batteries. Since the overall capacity in this system can include redox charge storage from the phosphaviologen species, and capacitance from the SWCNT additive, we tested a control battery with a SWCNT:PVDF electrode (PVDF: poly(vinylenedifluoride)). This control battery showed that only 6–9 mAh/g of the total capacity can be attributed to the SWCNTs, with the remaining capacity originating from the reversible reduction of **PY_2PV** (Supporting Information). Cyclic voltammetry and impedance spectroscopy on the fully assembled battery also indicate that 80–85 % of the total battery capacity stems from faradaic charge storage (i.e. stemming from the electrochemical reactions of **PY_2PV**) with the remainder coming from capacitance (Supporting Information). It should be noted that the capacity values reported herein represent the total capacity of the battery. The importance of the pyrene-unit physisorption to SWCNTs was studied in two ways: i) making electrodes using phosphaviologens with pendant methyl groups rather than pyrene (**M_2PV**) and ii) making electrodes using **PY_2PV** without SWCNTs, but rather casting **PY_2PV** into porous carbon. In both cases there was rapid degradation in capacity upon cycling, highlighting the importance of the pyrene:SWCNT interactions in preventing dissolution of the electrode and giving rise to the observed high stability of the electrode (Supporting Information). Typically, small molecules cannot be used in organic batteries due to their high solubility, in spite of their generally tailorable and advantageous redox properties. Tethering organic electroactive moieties to SWCNTs using pyrene is an effective method for preventing capacity decay by electrode dissolution. The investigated **PY_2PV**:SWCNT composites exhibit good rate performance, cycle stability, and material usage as a result of the pyrene:SWCNT interactions, as well as high voltages vs. Li/Li^+ as a result of the low-lying LUMO and the excellent electron-accepting properties of the phosphaviologen system.

3. Conclusions

Phosphaviologens can accept two electrons into their low-lying LUMO, allowing them to operate as a high voltage material in Li-ion hybrid batteries. Small-molecule organics traditionally do not work well in batteries due to their high solubility, however the phosphaviologen scaffold can be functionalized with peripheral pyrene groups allowing them to form composites with SWCNTs that prevent dissolution via attractive π-stacking interactions. Notably, this composite does not interfere with the favorable electrochemical performance of phosphaviologens, and the SWCNTs also act as the conductive additive in the electrode. This solubility-reducing composite imparts high cycle stability to the electrode and the conductive SWCNTs give rise to good rate performance. The phosphaviologen: SWCNT composites have a capacity of up to 53 mAh/g at 1 C, and retain their capacity after 500 cycles, showing no degradation upon repeated cycling. Compositing organic electroactive molecules with conductive SWCNTs using pyrene is thus a general strategy for improving lifetime and performance of organic electrode materials and holds promise for the myriad of organic small molecules that are not suitable for battery applications due to their solubility.

Experimental Section

General Considerations. $^{31}P\{^1H\}$ NMR, ^1H NMR, $^{19}F\{^1H\}$ NMR, and $^{13}C\{^1H\}$ NMR spectra were recorded on Bruker Fourier 300HD, or Bruker Avance (-II,-III) 400 MHz spectrometers. Chemical shifts were referenced to external 85 % H_3PO_4 (^{31}P), C_6F_6 (^{19}F) and external TMS (^1H, ^{13}C) or residual non-deuterated solvent peaks (^1H, ^{13}C). Mass spectra were run on a Finnigan SSQ 7000 spectrometer or a Bruker Daltonics AutoFlex III system. Optical spectroscopy was conducted using a Cary 5000 UV-vis spectrophotometer. Fluorescence spectroscopy was conducted using an Edinburgh Instruments FS5 spectrofluorometer. All electrochemical experiments were conducted on Metrohm Autolab PGSTAT204 potentiostat. Batteries were fabricated using an EL-Cell reusable coin cell apparatus.

Materials. All solvents were purchased from Sigma Aldrich, sparged with argon, dried over activated molecular sieves, and stored under argon atmosphere prior to use. Poly(vinylenedifluoride) (PVDF; Mw = 534,000) and $LiPF_6$ (99.99 % purity) were purchased from Sigma Aldrich. $TBAPF_6$ was purchased from Sigma Aldrich then recrystallized from ethanol and dried under vacuum before use. SWCNTs were purchased from Raymor and used as received. Lithium foil was purchased from Sigma Aldrich and stored under argon. NMR solvents were purchased from Sigma-Aldrich. 2,7-Diazadibenzophosphole oxide (**PV**) and dimethyl phosphaviologen (**M_2PV**) were prepared according to our previously reported procedures.[47]

Preparation of PY_2PV (Br). 2,7-Diazadibenzophosphole oxide (**PV**) (400 mg, 1.44 mmol) and 1-(bromomethyl)pyrene (2.57 g mg, 8.7 mmol) were dissolved in chloroform (100 mL). The mixture was left to stir at room temperature over 3 days. A dark precipitate formed and was collected via vacuum filtration. The crude ^1H NMR spectrum revealed mono-substituted product still remaining and the precipitate was sonicated in acetonitrile for 2 hrs. The remaining precipitate was collected via vacuum filtration to afford **PY_2PV (Br)** as a brown/black powder (669 mg, 80 % yield). ^1H NMR (400 MHz, DMSO-d_6) δ: 10.21 (d br., J = 4.0 Hz, 2H), 9.61 (d br., J = 8.0 Hz, 2H), 9.14 (d br., J = 8.0 Hz, 2H), 8.47–8.40 (m, 8H), 8.34–8.15 (m, 10H), 7.89–7.83 (m, 2H), 7.71–7.67 (m, 1H), 7.61–7.59 (m, 2H), 6.74 (s br., 4H) ppm. ^{13}C NMR (101 MHz, DMSO-d_6) δ:151.48, 150.99, 147.68, 144.37, 135.29, 132.49, 132.21, 131.37, 131.08, 130.90, 130.55, 129.93, 129.74, 129.40, 129.12, 128.83, 128.19, 127.88, 127.67, 127.30, 126.77, 126.54, 125.79, 125.51, 124.53, 124.04, 122.72, 62.69. ^{31}P NMR (162 MHz, DMSO-d_6) δ: 28.4 ppm.

Preparation of PY_2PV. Compound **PY_2PV (Br)** (669 mg, 0.77 mmol) was suspended in dry and degassed acetonitrile (20 mL). Methyl triflate (0.5 mL, 4.57 mmol) was added and the suspension was left

to stir overnight at room temperature. Volatiles were removed and the solid was taken up in deionized water. The water suspension was sonicated for 1 hr, followed by vacuum filtration to afford **PY_2PV (OTf)** as a grey-brown powder (750 mg, 97% yield). ^{1}H NMR (300 MHz, DMSO-d_6) δ: 10.21 (s br., *2*H), 9.59 (s br., *2*H), 9.12 (s br., 1H), 8.42–8.17 (m, 18H), 7.89–7.76 (m, 3H), 7.60 (s br., 2H), 6.72 (s br., 4H) ppm. ^{13}C NMR (76 MHz, DMSO-d_6) δ:150.96, 147.88, 147.63, 135.00, 134.16, 132.54, 132.29, 132.12, 131.12, 130.54, 129.91, 129.67, 129.54, 129.13, 127.70, 126.82, 126.54, 126.33, 125.81, 125.21, 124.58, 124.02, 122.60, 62.88. ^{31}P NMR (121 MHz, DMSO-d_6) δ: 28.6 ppm. ^{19}F NMR (282 MHz, DMSO-d_6) δ: 77.30 ppm. HRMS (ESI, m/z): [M + 1] calcd for: $C_{50}H_{33}N_2OP^+$, 739.2509; Found 739.2534.

Nanotube Functionalization. PY_2PV (12 mg, 0.013 mmol) was dissolved in acetonitrile (20 mL) and sonicated for 5 min. To this solution, the desired amount of SWCNTs was added and the entire suspension was sonicated for 1 hr. This resulted in a dark brown solution with very few visible solids. Subsequently, the volatiles were removed under vacuum to afford a black solid.

Electrode Preparation. PY_2PV:SWCNT composites were dissolved in *N*-methyl-2-pyrrolidone (NMP) at 20 mg/mL. The solution was sonicated for 15 minutes and stirred at 90 °C for 1 hour. A separate solution of 20 mg/mL of PVDF in NMP was prepared and stirred at 90 °C until it dissolved. Subsequently, a PVDF solution is added to the **PY_2PV**:SWCNT solution to create a 20 wt% PVDF 80 wt% **PY_2PV**:SWCNT composite. This solution is sonicated for 15 minutes and stirred at 90 °C for 1 hour. 0.1 mL of the slurry is evenly spread over the electrode (carbon-coated copper) and dried at 90 °C. The electrode is then dried under vacuum at 90 °C for 72 hours before being used in a battery. The total amount of material per electrode is around 2 mg, giving an areal density of 1 mg/cm^2.

Battery Testing. The battery is assembled using an EL-cell ECC-ref reusable test cell in a coin cell geometry using a lithium reference and 1.0 M $LiPF_6$ in TEGDME electrolyte. A lithium foil of diameter 18 mm was used as the anode, an 18 mm diameter glass fiber separator (EL-cell) was used to prevent short circuiting, and carbon-coated copper (EL-cell) was used as the cathodic current collector. Li coins were cut using an ECC Li-punch press and C/Cu coins were cut using an EL-cut from EL-cell. A battery architecture consisted of lithium foil : glass fiber impregnated with 0.35 mL electrolyte: **PY_2PV**:SWCNT/PVDF on carbon-coated Cu foil. The electrode was sealed in the cell inside of a glove box with an argon atmosphere before being used in cyclic voltammetry and battery cycling experiments. Current densities for different C-rates were calculated by assuming that **PY_2PV** has a specific capacity of 53 mAh/g.

Cyclic voltammetry. Cyclic voltammetry was conducted on a 10 mg/mL solution in dry, degassed acetonitrile containing 0.1 M $TBAPF_6$. A typical three-electrode cell was used with glassy carbon as a working electrode, Pt wire as a counter electrode, and Ag/AgCl as a reference electrode.

Acknowledgements

Financial support by the Natural Sciences and Engineering Research Council of Canada (NSERC) and the Canada Foundation for Innovation is gratefully acknowledged. M.S. thanks NSERC for a graduate scholarship, C.R.B. would like to acknowledge a York Science Fellowship, and T.B. thanks the Canada Research Chairs program for support. We would also like to thank J. Manion for obtaining the AFM data and Dr. S. Morin for her help with the conductivity measurements.

Keywords: viologen · phosphorus heterocycles · energy storage · nanotubes · phosphaviologen

[1] B. C. Melot, J. M. Tarascon, *Acc. Chem. Res.* **2013**, *46*, 1226–1238.
[2] D. Larcher, J. M. Tarascon, *Nat. Chem.* **2014**, *7*, 19–29.
[3] R. Guduru, J. Icaza, *Nanomaterials* **2016**, *6*, 41.
[4] J. B. Goodenough, Y. Kim, *Chem. Mater.* **2010**, *22*, 587–603.
[5] N. S. Ergang, J. C. Lytle, H. Yan, A. Stein, *J. Electrochem. Soc.* **2005**, *152*, A1989-A1995.
[6] Z. Liu, X. Yuan, S. Zhang, J. Wang, Q. Huang, N. Yu, Y. Zhu, L. Fu, F. Wang, Y. Chen, Y. Wu, *NPG Asia Mater.* **2019**, *11*, 12.
[7] T. B. Schon, B. T. McAllister, P.-F. Li, D. S. Seferos, *Chem. Soc. Rev.* **2016**, *45*, 6345–6404.
[8] J. Xie, Q. Zhang, *J. Mater. Chem. A* **2016**, *4*, 7091–7106.
[9] A. Mauger, C. Julien, A. Paolella, M. Armand, K. Zaghib, *Materials* **2019**, *12*, 1770.
[10] K. Xiao, D. Jiang, R. Amal, D.-W. Wang, *Adv. Mater.* **2018**, *30*, 1800400.
[11] L. Bießmann, L. P. Kreuzer, T. Widmann, N. Hohn, J.-F. Moulin, P. Müller-Buschbaum, *ACS. Appl. Mater. Interfaces* **2018**, *10*, 9865–9872.
[12] K. Oka, R. Kato, K. Oyaizu, H. Nishide, *Adv. Funct. Mater.* **2018**, *28*, 1805858.
[13] H. Tokue, T. Murata, H. Agatsuma, H. Nishide, K. Oyaizu, *Macromolecules*, **2017**, *50*, 1950–1958.
[14] Y. Lu, Q. Zhang, L. Li, L. Z. Niu, J. Chen, *Chem* **2018**, *4*, 2786–2813.
[15] Y. Liang, Y. Yao, *Joule* **2018**, *2*, 1690–1706.
[16] C. S. Sevov, R. E. M. Brooner, E. Chénard, R. S. Assary, J. S. Moore, J. Rodríguez-López, M. S. Sanford, *J. Am. Chem. Soc.* **2015**, *137*, 14465–14472.
[17] G. Dai, X. Wang, Y. Qian, Z. Niu, X. Zhu, J. Ye, Y. Zhao, X. Zhang, *Energy Storage Mater.* **2019**, *16*, 236–242.
[18] S. Muench, A. Wild, C. Friebe, B. Häupler, T. Janoschka, U. S. Schubert, *Chem. Rev.* **2016**, *116*, 9438–9484.
[19] N. Patil, M. Aqil, A. Aqil, F. Ouhib, R. Marcilla, A. Minoia, R. Lazzaroni, C. Jérôme, C. Detrembleur, *Chem. Mater.* **2018**, *30*, 5831–5835.
[20] T. Janoschka, M. D. Hager, U. S. Schubert, *Adv. Mater.* **2012**, *24*, 6397–6409.
[21] K. Nakahara, K. Oyaizu, H. Nishide, *Chem. Lett.* **2011**, *40*, 222–227.
[22] T. Suga, H. Ohshiro, S. Sugita, K. Oyaizu, H. Nishide, *Adv. Mater.* **2009**, *21*, 1627–1630.
[23] K. Oyaizu, H. Nishide, *Adv. Mater.* **2009**, *21*, 2339–2344.
[24] M. E. Speer, M. Kolek, J. J. Jassoy, J. Heine, M. Winter, P. M. Bieker, B. Esser, *Chem. Commun.* **2015**, *51*, 15261–15264.
[25] M. Kolek, F. Otteny, P. Schmidt, C. Mück-Lichtenfeld, C. Einholz, J. Becking, E. Schleicher, M. Winter, P. Bieker, B. Esser, *Energy Environ. Sci.* **2017**, *10*, 2334–2341.
[26] F. Otteny, M. Kolek, J. Becking, M. Winter, P. Bieker, B. Esser, *Adv. Energy Mater.* **2018**, *8*, 1802151.
[27] L. Chen, C. R. Bridges, G. Gao, T. Baumgartner, X. He, *ACS Appl. Energy Mater.* **2019**, *2*, 7315–7320.
[28] N. Patil, A. Aqil, F. Ouhib, S. Admassie, O. Inganäs, C. Jérôme, C. Detrembleur, *Adv. Mater.* **2017**, *29*, 1703373.
[29] H. Wu, S. A. Shevlin, Q. Meng, W. Guo, Y. Meng, K. Lu, Z. Wei, Z. Guo, *Adv. Mater.* **2014**, *26*, 3338–3343.
[30] T. Liu, K. C. Kim, B. Lee, Z. Chen, S. Noda, S.-S. Jang, S. W. Lee, *Energy Environ. Sci.* **2017**, *10*, 205–215.
[31] T. B. Schon, A. J. Tilley, C. R. Bridges, M. B. Miltenburg, D. S. Seferos, *Adv. Funct. Mater.* **2016**, *26*, 6896–6903.
[32] N. Hergué, B. Ernould, A. Minoia, R. Lazzaroni, J.-F. Gohy, P. Dubois, O. Coulembier, *Batteries & Supercaps* **2018**, *1*, 102–109; Supercaps **2018**, 1, 102–109.
[33] M. Stolar, C. Reus, T. Baumgartner, *Adv. Energy Mater.* **2016**, *6*, 1600944.
[34] M. Stolar, J. Borau-Garcia, M. Toonen, T. Baumgartner, *J. Am. Chem. Soc.* **2015**, *137*, 3366–3371.
[35] M. Stolar, T. Baumgartner, *Chem. Commun.* **2018**, *54*, 3311–3322.
[36] A. Jouhara, E. Quarez, F. Dolhem, M. Armand, N. Dupré, P. Poizot, *Angew. Chem.* **2019**, *131*, 15827–15831; *Angew. Chem. Int. Ed.* **2019**, *58*, 15680–15684.
[37] L. Cao, S. Sadaf, S. M. Beladi-Mousavi, L. Walder, *Eur. Polym. J.* **2013**, *49*, 1923–1934.
[38] M. Yao, H. Sano, H. Ando, T. Kiyobayashi, *Sci. Rep.* **2015**, *5*, 10962.
[39] G. Li, B. Zhang, J. Wang, H. Zhao, W. Ma, L. Xu, W. Zhang, K. Zhou, Y. Du, G. He, *Angew. Chem.* **2019**, *131*, 8556–8560; *Angew. Chem. Int. Ed.* **2019**, *58*, 8468–8473.

[40] T. Liu, X. Wei, Z. Nie, V. Sprenkle, W. Wang, *Adv. Energy Mater.* **2015**, *6*, 1501449.
[41] B. Hu, Y. Tang, J. Luo, G. Grove, Y. Guo, T. L. Liu, *Chem. Commun.* **2018**, *54*, 6871–6874.
[42] C. DeBruler, B. Hu, J. Moss, X. Liu, J. Luo, Y. Sun, T. L. Liu, *Chem* **2017**, *3*, 961–978.
[43] N. Sano, W. Tomita, S. Hara, C.-M. Min, J.-S. Lee, K. Oyaizu, H. Nishide, *ACS Appl. Mater. Interfaces* **2013**, *5*, 1355–1361.
[44] C. Ehli, G. M. A. Rahman, N. Jux, D. Balbinot, D. M. Guldi, F. Paolucci, M. Marcaccio, D. Paolucci, M. Melle-Franco, F. Zerbetto, S. Campidelli, M. Prato, *J. Am. Chem. Soc.* **2006**, *128*, 11222–11231.
[45] P. Salice, A. Gambarin, N. Daldosso, F. Mancin, E. Menna, *J. Phys. Chem. C* **2014**, *118*, 27028–27038.
[46] T. Umeyama, J. Baek, Y. Sato, F. Abou-Chahine, H. Lemmetyinen, K. Suenaga, N. V. Tkachenko, H. Imahori, *Nat. Commun.* **2015**, *6*, 7732.
[47] S. Durben, T. Baumgartner, *Angew. Chem.* **2011**, *123*, 8096–8100; *Angew. Chem. Int. Ed.* **2011**, *50*, 7948–7952.

Manuscript received: October 29, 2019
Revised manuscript received: November 29, 2019
Version of record online: December 19, 2019